



# Superior *in vitro* anticancer effect of biomimetic paclitaxel and triptolide co-delivery system in gastric cancer

Siwan Wang<sup>1,Δ</sup>, Hui Jiang<sup>1,Δ</sup>, Jia Wang<sup>1,Δ</sup>, Haisi Wu<sup>1</sup>, Ting Wu<sup>1</sup>, Mengnan Ni<sup>1</sup>, Qianqian Zhao<sup>1</sup>, You Ji<sup>1</sup>, Ziting Zhang<sup>3</sup>, Chunming Tang<sup>1,✉</sup>, Huae Xu<sup>1,2,✉</sup>

<sup>1</sup>Department of Pharmaceutics, School of Pharmacy, Nanjing Medical University, Nanjing, Jiangsu 211166, China;

<sup>2</sup>Jiangsu Key Laboratory of Molecular and Translational Cancer Research, Affiliated Cancer Hospital of Nanjing Medical University, Jiangsu Cancer Hospital, Jiangsu Institute of Cancer Research, Nanjing, Jiangsu 210009, China;

<sup>3</sup>Department of Geriatric Gastroenterology, the First Affiliated Hospital of Nanjing Medical University, Nanjing, Jiangsu 210029, China.

## Abstract

As a well-known anticancer drug, paclitaxel (PTX), a first-line chemotherapeutic agent, remains unsatisfactory for gastric cancer therapy. It is reported that triptolide (TPL) could enhance the anti-gastric cancer effect of PTX. Considering the poor solubility of both drugs, we developed a red blood cell membrane-biomimetic nanosystem, an emerging tool in drug delivery, to co-load paclitaxel and triptolide (red blood cell membrane coated PTX and TPL co-loaded poly(lactic-co-glycolic acid) [PLGA] nanoparticles, RP(P/T)). The successful preparation was confirmed in terms of particle size, morphology, and surface markers assays. This biomimetic system could prolong circulation and escape immune surveillance. And these properties were verified by stability, *in vitro* drug release, and cellular uptake assays. Moreover, the MTT and colony formation assays demonstrated the superior anti-proliferation effect of the RP(P/T) to free drugs. The enhanced antitumor effects of RP(P/T) on migration and invasion were also evaluated by wound-healing and transwell assays. Overall, the bionic co-delivery nanoplatform with improved efficacy *in vitro* is a promising therapy for gastric cancer.

**Keywords:** paclitaxel, triptolide, red-blood-cell membrane, gastric cancer

## Introduction

Gastric cancer is one of the most common cancers in the world, ranking 5th in the incidence of malignant tumors and the 3rd in mortality, respectively<sup>[1–3]</sup>. According to National Comprehensive Cancer Network (NCCN) 2020 gastric cancer guidelines<sup>[4–5]</sup>, Paclitaxel (PTX) is one of the main components of the

first-line chemotherapy regimens. PTX is a microtubule stabilizer extracted from the *Pacific yew tree* and could disturb mitosis by promoting the polymerization of microtubule and inhibiting the depolymerization of the microtubule<sup>[6]</sup>.

Nevertheless, the performance of PTX in clinical chemotherapy does not meet the expectation owing to its drug resistance. Previous studies discovered that

<sup>Δ</sup>These authors contributed equally to this work.

<sup>✉</sup>Corresponding authors: Huae Xu and Chunming Tang, Department of Pharmaceutics, School of Pharmacy, Nanjing Medical University, 101 Longmian Avenue, Nanjing, Jiangsu 211166, China. E-mails: [xuhuae@njmu.edu.cn](mailto:xuhuae@njmu.edu.cn) and [cmrtang@njmu.edu.cn](mailto:cmrtang@njmu.edu.cn).

Received: 28 June 2021; Revised: 07 July 2021; Accepted: 12 July 2021; Published online: 28 July 2021

CLC number: R318.08, Document code: A

The authors reported no conflict of interests.

This is an open access article under the Creative Commons Attribution (CC BY 4.0) license, which permits others to distribute, remix, adapt and build upon this work, for commercial use, provided the original work is properly cited.

combined chemotherapy is an excellent option to make cancer cells restore the sensitivity to PTX<sup>[7-9]</sup>. Triptolide (TPL), a natural product isolated from *Tripterygium wilfordii* Hook F, is a reported diterpenoid exhibiting the inhibitory effect on various tumor cells, such as gastrointestinal cancer, breast cancer, and prostate cancer<sup>[10]</sup>. What's more, TPL could also improve the therapeutic outcome of PTX<sup>[7]</sup>.

However, the combinational application of PTX and TPL in the clinic is limited by their poor solubility. Commercial paclitaxel (Taxol), needs to be dissolved in a mixture of polyoxyethylene castor oil and anhydrous ethanol, which may trigger allergic reactions or hypersensitivity reactions<sup>[11]</sup>. Similarly, the poor water solubility of TPL and its extremely high systemic toxicity in the liver and heart also limit its clinical use<sup>[10]</sup>. In this regard, it is of great significance to develop a novel drug delivery system of PTX and TPL.

The application of nano-drug delivery systems has shed light on the delivery of chemotherapeutics. These systems can lower toxicity, control drug release, and improve tumor accumulation<sup>[12]</sup>. Researchers have explored diverse nanocarriers to load PTX, such as liposomes, polymers, *etc*<sup>[13-14]</sup>. Earlier studies of our research group have successfully constructed a series of PTX loaded nanoparticles with poly(lactic-co-glycolic acid) (PLGA), poly( $\epsilon$ -caprolactone)-poly(ethylene glycol) (PCL-PEG), and "carrier-free" nanofibers as drug carriers<sup>[8-9,15]</sup>. However, there are several drawbacks in these systems, including high immunogenicity, rapid clearance by the body's reticuloendothelial system, and premature drug release during blood circulation<sup>[16-17]</sup>.

The biomimetic system has been a promising strategy to address these limitations. In 2011, Zhang's group first reported a bionic nano-drug delivery system, which creatively camouflaged polymeric nanoparticles with red blood cell (RBC) membranes<sup>[18]</sup>. Nanoparticles wrapped with red blood cell membrane can not only evade the clearance of immune system but also exhibit the specialties of low immunogenicity, long circulation, good biocompatibility, biodegradability, high drug loading capacity, *etc*<sup>[19-20]</sup>. Recently, the biomimetic nano-delivery system has become a focus of research and one of the most promising frontiers of nano-delivery.

Inspired by this, we designed an efficient, low-toxicity, mass-producible, and quality-controlled biomimetic co-delivery drug delivery system to load paclitaxel and triptolide for the treatment of gastric cancer, with promising clinical applications. This system comprised two components: (1) PTX and TPL co-loaded PLGA nanoparticles (P(P/T)) for drug

retention and antitumor effects; (2) Red blood cell membrane (RBCM)-based shell for evasion of immune surveillance and extension of blood circulation.

## Materials and methods

### Reagents

Paclitaxel ( $\geq 99.0\%$ ) and coumarin-6 ( $\geq 98.0\%$ ) were obtained from Shanghai Aladdin Biochemical Technology, China. Triptolide ( $\geq 98.0\%$ ) was purchased from Nantong Feiyu Biological Technology, China. Polyvinyl alcohol (PVA, MW 15 000 kDa; hydrolyzed 87%–89%) was purchased from Energy Chemical, China. RIPA lysis buffer and sodium dodecyl sulfate-polyacrylamide gel were obtained from Epizyme, China. Coomassie Brilliant Blue G-250, BCA protein assay kit, Coomassie Blue Staining Solution, antifade mounting medium with DAPI, and 3-(4,5-dimethyl-2-thiazolyl)-2,5-diphenyl-2-H-tetrazolium bromide (MTT) were purchased from Beyotime, China. Dimethyl sulfoxide (DMSO) was purchased from Sigma-Aldrich, China. Phosphate buffered saline (PBS) solution was obtained from Cytiva, USA. Transwell plates were obtained from Corning Costar, USA. Crystalline violet staining solution and 4% paraformaldehyde were purchased from Solarbio, China.

### Cell culture

Based on the universalities in the gastric cancer preclinical study, we chose the poorly differentiated gastric cancer cell lines MNK-45, BGC-823, and the moderately-poorly differentiated gastric adenocarcinoma cell line SGC-7901 in this study. MNK-45, BGC-823, and SGC-7901 cells, obtained from Cell Bank of Type Culture Collection of the Chinese Academy of Sciences (China), were cultured in RPMI-1640 (Biological Industries, Israel). Mouse macrophage cell line RAW264.7 was purchased from FuHeng Cell Center, China, and cultured in DMEM (high glucose, Biological Industries). All the cells were cultured with 10% fetal bovine serum (FBS, Biological Industries) at 37 °C in a 5% CO<sub>2</sub> atmosphere.

### General measurement

Dynamic light scattering (DLS) was conducted by BeNano90Zeta (Bettersize, China). OD value was observed by TECAN Infinite F50 microplate reader, Switzerland. Probe Ultrasonic Processor was purchased from Nanjing Aptio Instruments Manu-

facture, China. Transmission electron microscopy (TEM) was performed using JEOL JEM-1010 electron microscope, Japan. The drug concentration was determined by Shimadzu CBM-20A high-performance liquid chromatography (HPLC; Japan). *In vitro* drug release was performed in a constant temperature oscillating culture shaker (Zhicheng, China).

### **Preparation of red blood cell membrane-coated paclitaxel and triptolide co-loaded PLGA nanoparticles**

#### *Isolation and extraction of red blood cell membranes*

Fresh whole blood taken from male BALB/c mice was centrifuged (600 g, 5 minutes, 4 °C) to remove the plasma and yellow-brown buffy coat. Obtained red blood cells were washed 3 times with pre-chilled 1× PBS, then lysed in hypotonic 0.25× PBS for 30 minutes on ice. Hemoglobin was removed by centrifugation at 2000 g for 15 minutes at 4 °C. The red blood cells were collected and subjected to repeated freeze-thaw cycles to obtain red blood cell membranes. Then the purified red blood cell membranes were resuspended with 1× PBS and stored at -80 °C. All experimental procedures were approved by the Nanjing Medical University Ethics Committee for Animal Laboratory Research and followed the guidelines of ethical regulations for institutional animal care and use in Nanjing Medical University.

#### *Preparation of red blood cell membrane vesicles*

The red blood cell membranes were centrifuged at 8000 g for 8 minutes at 4 °C and suspended in water and sonicated in a capped glass vial for 5 minutes using a bath sonicator. The supernatant was the solution of desired red blood cell membrane vesicles.

#### *Preparation of P(P/T)*

P(P/T) were prepared by the method reported by Tang *et al* using a modified conventional oil-in-water (O/W) single emulsion solvent evaporation method<sup>[21]</sup>. Briefly, a certain amount of PLGA, paclitaxel, and triptolide were dissolved in dichloromethane as the organic phase. The mixture was emulsified with 8 mL of the PVA aqueous solution (1 wt %) using a probe-type sonicator at 150 w for 5 minutes in ice bath. The resulting suspension was stirred for 4 hours at room temperature to evaporate the organic solvent and was subsequently centrifuged at 15 000 g for 30 minutes. P(P/T) were washed three times with distilled water to remove the residual PVA and resuspended in 1× PBS. The coumarin-6 labeled PLGA nanoparticles (C6-NPs) were prepared with the similar method described

above except using 0.1 wt% coumarin-6 instead of paclitaxel and triptolide.

#### *Preparation of red blood cell membrane-encapsulated P(P/T)*

The red blood cell membrane-cloaked nanoparticles were fabricated by a sonication method. The erythrocyte membrane vesicles were mixed with P(P/T) and placed in a capped glass vial. Then the mixture was sonicated for 5 minutes in an ice-water bath to obtain red blood cell membrane-cloaked paclitaxel and triptolide co-loaded PLGA nanoparticles (RP(P/T)). The red blood cell membrane-cloaked C6-NPs (R-C6-NPs) were prepared with the similar method described above except using C6-NPs instead of P(P/T).

#### *In vitro* release of drug from the RP(P/T)

One mL of P(P/T) or RP(P/T) was added into a dialysis tube (3.5K MWCO) embedded into 50 mL of the PBS buffer solution (pH 6.5) containing 1% (w/v) Tween 80 and gently shaken at 100 rpm in a shaker at 37 °C. At predetermined time intervals, one mL of the medium was drawn out and replenished with an equal volume of fresh medium. Then, the PTX and TPL were extracted, and the concentrations of PTX and TPL were determined by HPLC.

#### **Characterization of RP(P/T)**

The particle size and surface zeta potential of P(P/T) and RP(P/T) were measured by a laser particle size analyzer (BeNano90Zeta), respectively. The morphologies were determined by transmission electron microscopy. The samples were prepared by contacting the nanoparticle droplets at a concentration of 100 µg/mL with copper grids for 3 minutes, removing the excess droplets, and staining by 1% phosphotungstic acid for 60 seconds before the TEM studies. P(P/T) and RP(P/T) were added into 1× PBS and 100% FBS to examine their stability. The change of particle sizes within 7 days (1× PBS) and 24 hours (100% FBS) was monitored by DLS.

Coomassie blue staining was employed to identify the proteins on RP(P/T). Briefly, the samples containing equivalent total proteins measured by BCA protein assay kit were added to the 10% SDS-polyacrylamide gel to separate different molecular weights of proteins. Subsequently, the resulting polyacrylamide gel was stained with Coomassie brilliant blue and imaged.

#### **Analysis of drug loading and encapsulation efficiency**

The drug loading and encapsulation efficiency of

paclitaxel and triptolide were quantified by HPLC. Lyophilized PLGA microspheres (10 to 15 mg) were dissolved with 0.5 mL dichloromethane, and then 0.5 mL methanol was added. After violent agitation, the suspension was centrifuged (2000 g, 5 minutes) and 200  $\mu$ L supernate was extracted for HPLC analysis. The HPLC analysis was conducted with C-18 RP column, methanol as buffer A, water as buffer B, and the elution gradient being 75% to 25% (paclitaxel) and 60% to 40% (triptolide)/15 minutes. The quantity of paclitaxel and triptolide was evaluated by UV absorption at 227 nm and 218 nm, respectively. And the drug loading and encapsulation efficiency were calculated as follows:

$$\text{DLE} = \frac{m'_{\text{drug}}}{m'_{\text{ms}}} \times 100\% \quad (1)$$

$$\text{EE} = \frac{m_{\text{ms}} \times \text{DLE}}{m_{\text{drug}}} \times 100\% \quad (2)$$

where DLE is drug loading efficiency,  $m'_{\text{drug}}$  is the mass of drug measured in the sample nanoparticles,  $m'_{\text{ms}}$  is the mass of the sample nanoparticles used to determine the drug loading; EE is encapsulation efficiency,  $m_{\text{ms}}$  is the mass of all the nanoparticles obtained in each experiment and  $m_{\text{drug}}$  is the total mass of drug used in each experiment.

### ***In vitro* antitumor activity**

#### *Cellular uptake of the red blood cell membrane coated PLGA nanoparticles*

RAW264.7 and MNK-45 cells were cultured in confocal dishes (Sorfa, China) for 24 hours. After that, the cells were treated with C6-NPs or R-C6-NPs for 2 hours. Then, the cells were washed with 1 $\times$  PBS for 3 times and fixed in 4% paraformaldehyde for 15 minutes. Next, the cells were stained with an antifade mounting medium with DAPI. Phagocytosis of RAW264.7 and MNK-45 cells was observed by confocal laser scanning microscopy (CLSM; ZEISS LSM800, Germany).

#### *In vitro* cytotoxicity

*In vitro* cytotoxicity of paclitaxel, triptolide, P(P/T), and RP(P/T) were evaluated by MTT assay. The gastric tumor cells were seeded on 96-well culture plates with RPMI-1640 medium at a density of 5000 cells per well and incubated in a 5% CO<sub>2</sub> atmosphere at 37 °C for 24 hours. The cells were then incubated with different concentrations of paclitaxel, triptolide, P(P/T), and RP(P/T) for 24, 48, and 72 hours, respectively. Afterward, 10  $\mu$ L MTT solution (5 mg/mL) was added to each well. After incubation for 4 hours, 150  $\mu$ L DMSO was added to each well. The

absorbance was detected at 492 nm using a microplate reader after shaking for 10 minutes.

#### *Colony formation assay*

For colony formation assay, 500 cells were seeded into six-well plates overnight and then treated with PBS, PTX, TPL, PTX+TPL (the PTX:TPL ratio was 1:0.5), P(P/T), and RP(P/T) for 24 hours. Next, the supernatant was discarded, and the cells were cultured in a fresh culture medium. The medium was changed every 3 days. After two weeks, the plate was washed with 1 $\times$  PBS for 3 times and fixed with 4% paraformaldehyde for 15 minutes and stained with crystal violet for 15 minutes. Finally, photos were taken using microscopy.

#### *Cell wound healing assay*

SGC-7901 cells were seeded into 6-well plates overnight. The cell monolayer was subsequently scratched with a 200  $\mu$ L pipette tip. Next, cells were incubated with various drug formulations in serum-free media for 24 and 48 hours. Cell images were subsequently captured under a microscope. The migration rate (MR) was considered as migration ability and was calculated as below:

$$\text{MR} = \frac{\text{original wound area} - \text{area at detection}}{\text{original wound area}} \times 100\% \quad (3)$$

#### *Cell migration assay*

Cells were cultured in a transwell plate with 200  $\mu$ L serum-free medium in the upper after incubated with different drugs for 24 hours, and 500  $\mu$ L medium containing 10% fetal bovine serum in the lower. After incubation for another 24 hours, the cells that did not migrate through the well were removed. The migrating cells at the lower surface were stained with 0.5% crystal violet. Migrating cells were then photographed under a microscope. The Invasion rate (IR) was considered as transwell migration ability and was calculated as below:

$$\text{IR} = \frac{N_{\text{lower}}}{N_{\text{total}}} \times 100\% \quad (4)$$

where  $N_{\text{lower}}$  is the number of cells in the lower chamber,  $N_{\text{total}}$  is the total number of input cells.

### **Statistical analysis**

All statistical analyses were performed using the Prism software (Prizm 7.0, GraphPad Software, USA). All the results are expressed as mean  $\pm$  standard deviation ( $n \geq 3$ ). Differences among groups were analyzed by Student's *t*-test.  $P < 0.05$  was considered statistically significant.

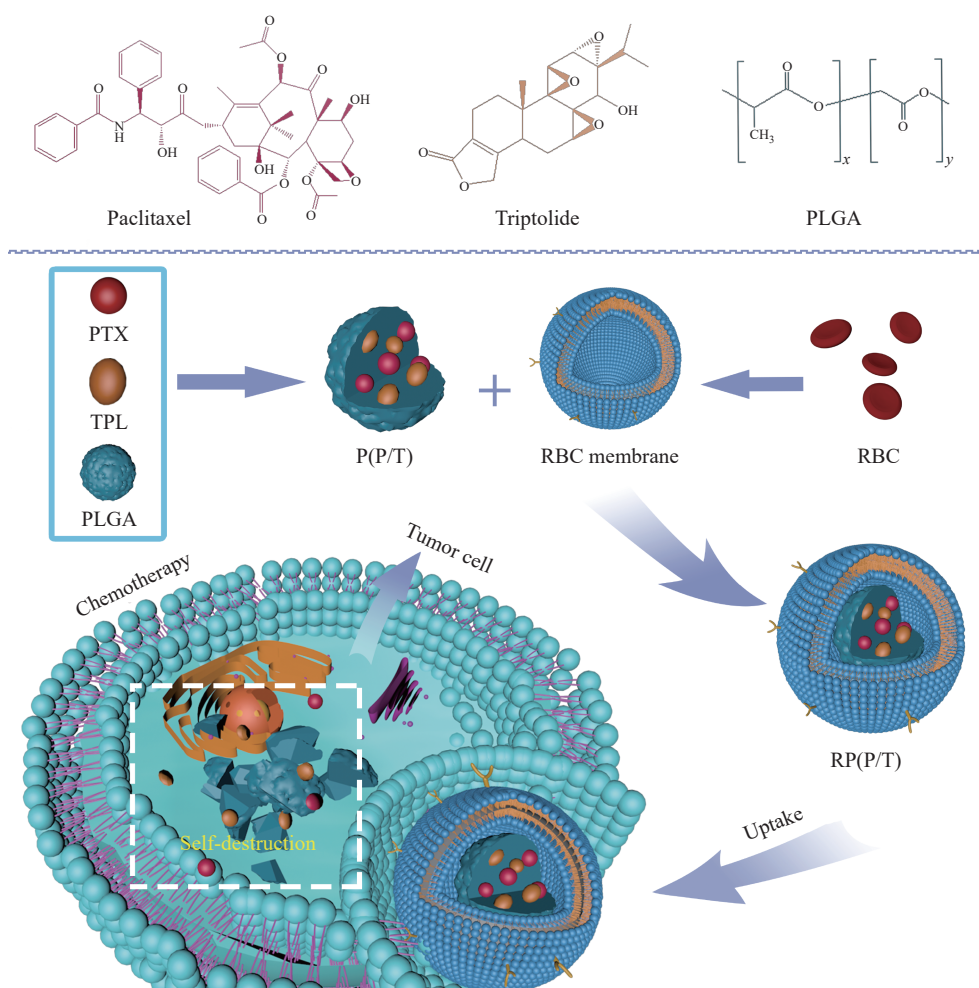


**Fig. 1** Preparation of RBCM coated PTX and TPL co-loaded PLGA nanoparticles for cancer therapy. The preparation of RBCM coated PTX and TPL co-loaded PLGA nanoparticles (RP(P/T)) was composed of two parts: co-loading PTX and TPL into PLGA to obtain P(P/T); coating the P(P/T) with RBCM. When endocytosed by cancer cells, RP(P/T) could inhibit the growth of cancer cells by a synergistic effect. RBCM: red blood cell membrane; PTX: paclitaxel; TPL: triptolide; P(P/T): PTX and TPL co-loaded PLGA nanoparticles.

## Results

### Preparation of RBCM coated PTX and TPL co-loaded nanoparticles

The preparation of RP(P/T) consists of two main steps: internal particle preparation and surface membrane encapsulation. As indicated in **Fig. 1**, the inner layer P(P/T) was first prepared. Later, the red blood cell membrane was wrapping onto the surface *via* sonication in an ice water bath. Afterward, RP(P/T) would be ingested by tumor cells, and both drugs would be released inside the cytoplasm, thereby inducing apoptosis.

### Drug loading and encapsulation efficiency

The optimizing prescription was carried out with the above two factors as well as the reported optimal synergy ratio<sup>[7]</sup>. A dosage ratio of 1:0.5 was selected for paclitaxel and triptolide to prepare the co-delivery system and conduct subsequent experiments. The drug

loading efficiency was 1.56% of paclitaxel and 4.09% of triptolide; the encapsulation efficiency of paclitaxel and triptolide was 15.8% and 92.7%, respectively (**Table 1**).

### Characterization of RP(P/T)

The size of RP(P/T) was characterized by DLS (**Fig. 2A** and **B**). The prepared P(P/T) has a particle

PTX/ TPL	DL of PTX (%)	EE of PTX (%)	DL of TPL (%)	EE of TPL (%)
0.5:0.5	0.66	22.3	3.64	89.7
1.0:0.5	1.56	15.8	4.09	92.7
1.0:1.0	0.36	6.2	8.77	93.9
0.5:1.0	0.57	18.0	8.11	92.1

PTX: paclitaxel; TPL: triptolide; DLE: drug loading efficiency; EE: encapsulation efficiency.

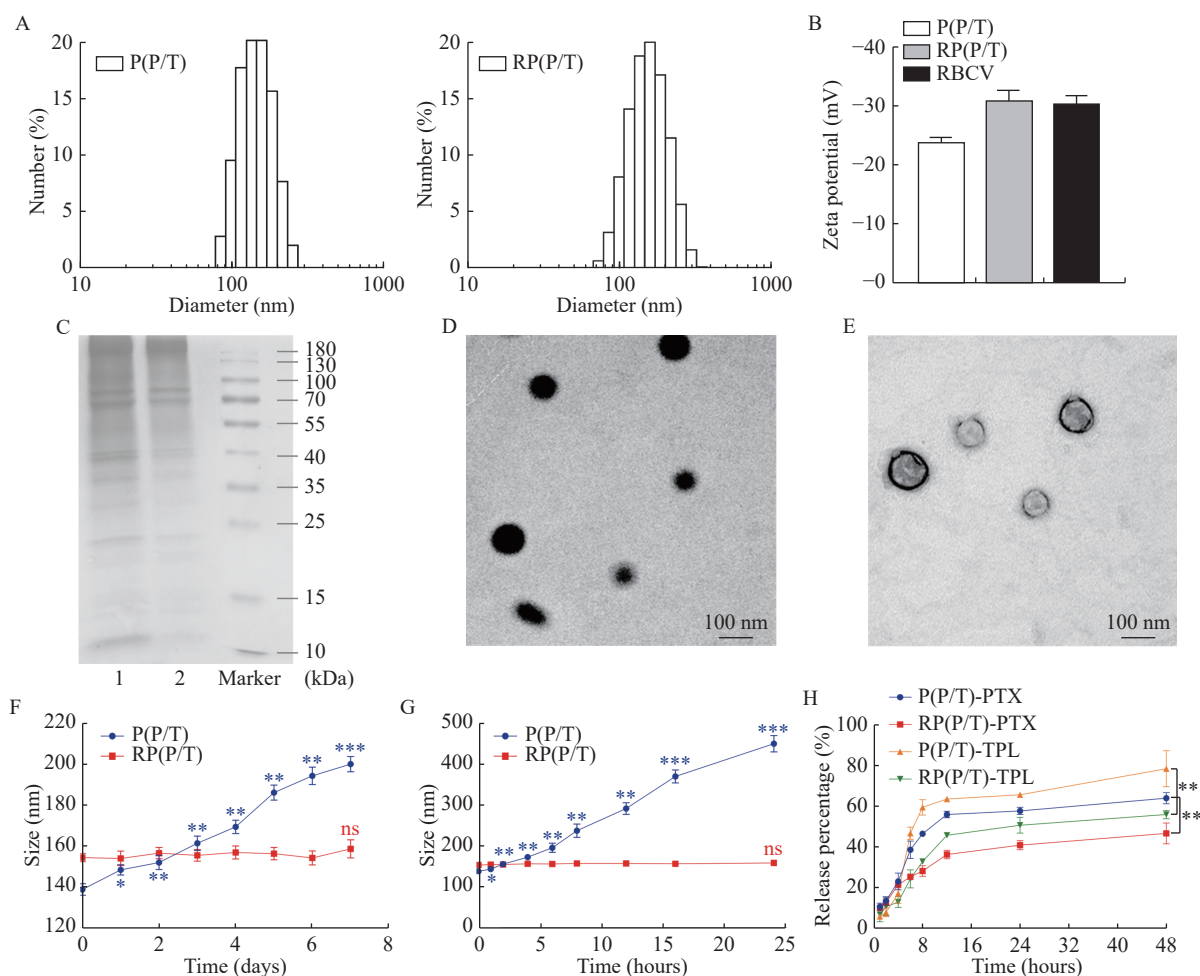


**Fig. 2 Characterization of RP(P/T).** A: Particle size distribution of P(P/T) and RP(P/T) measured by dynamic light scattering. B: Zeta potential of P(P/T) and RP(P/T). Error bars indicate SD ( $n=5$ ). C: SDS-PAGE analysis of RBCVs (lane 1) and RP(P/T) (lane 2). D and E: Representative TEM images of P(P/T) (D) and RP(P/T) (E). Scale bar, 100 nm. F and G: Stability of P(P/T) and RP(P/T) in PBS (F) and 100% FBS (G) monitored by dynamic light scattering at 37 °C. Error bars indicate SD ( $n=3$ ). Differences between different time points and the zero-time point were analyzed by Student's *t*-test. \* $P<0.05$ , \*\* $P<0.01$ , \*\*\* $P<0.001$ . H: *In vitro* release of paclitaxel and triptolide from P(P/T) and RP(P/T) in PBS (pH 6.5) was measured by high-performance liquid chromatography. P(P/T)- and RP(P/T)-PTX represent the drug release of PTX from P(P/T) and RP(P/T), respectively. P(P/T)- and RP(P/T)-TPL represent the drug release of TPL from P(P/T) and RP(P/T), respectively. Differences among groups were analyzed by Student's *t*-test. \* $P<0.05$ , \*\* $P<0.01$ , \*\*\* $P<0.001$ . P(P/T): PTX and TPL co-loaded PLGA nanoparticles; RP(P/T): red blood cell membrane coated PTX and TPL co-loaded PLGA nanoparticles; PLGA: poly(lactic-co-glycolic acid); PTX: paclitaxel; TPL: triptolide.

size of about 139 nm, and the size increased by approximately 15 nm to 154 nm after coating the red blood cell membrane. Furthermore, the zeta potential of RP(P/T) was about  $-30$  mV (**Fig. 2B**).

SDS-PAGE was then performed to verify that RBC membrane proteins, including CD47 and an array of complement regulatory proteins, were present in the biomimetic nanoparticles (**Fig. 2C**). Lane 1 and 2 represent the red blood cell membrane vesicles (RBCVs) and RP(P/T), respectively. The two samples displayed similar protein brands, indicating that the membrane proteins were preserved during preparation and successfully modified on the nanoparticles.

In addition, the morphological features of the two nanoparticles were characterized by TEM. The prepared inner core P(P/T) had a spherical structure

with a particle size of about 100 nm, which is slightly smaller than the size measured by DLS (**Fig. 2D**). The electron micrographs of RP(P/T) after coating the red blood cell membrane exhibited a particle size of about 110 nm, slightly larger than that of the naked PLGA nanoparticles (**Fig. 2E**). In addition, RP(P/T) showed a core-shell spherical structure compared to naked P(P/T), and a cell-membrane structure could be observed around the RP(P/T). The thickness of the membrane (ghost vesicles) shell was about 10 nm. The above findings confirmed the successful wrapping of the red blood cell membrane around the R(P/T) surface.

#### ***In vitro* stability of RP(P/T)**

We investigated the stability of P(P/T) and RP(P/T)

by monitoring their size and size distribution in two simulated physiological buffers, PBS (pH 7.4) (**Fig. 2F**) and 100% FBS (**Fig. 2G**). The particle size of RP(P/T) was almost constant in both buffer systems, indicating that RP(P/T) had superior stability in both PBS and FBS. In comparison, the size P(P/T) was unstable and tended to aggregate and precipitate at the same condition. The results illustrated that the membrane modification could significantly improve the stability of nanoparticles due to the excellent biocompatibility of red blood cells. In other words, the red blood cell membrane coating could protect nanoparticles and prolong blood circulation.

### ***In vitro* release of paclitaxel and triptolide from RP(P/T)**

Since the drug release from the delivery system is an essential property for its application in cancer therapy. We examined the drug release ability of this biomimetic delivery system in pH 6.5 buffer, mimicking the acidic tumor microenvironment.

The release of drugs from uncoated nanoparticles was significantly faster than RP(P/T) (**Fig. 2H**). This may be due to the protection of the red blood cell membrane. The presence of RBCM hindered the

release of the drugs and suggested an excellent sustained-release performance.

The above results indicated that the red blood cell membrane was successfully coated on the nanoparticle surface in RP(P/T). In summary, we successfully prepared nanoparticles co-loaded with paclitaxel and triptolide wrapped around by the red blood cell membrane with uniform particle size and excellent stability.

### ***In vitro* cellular uptake of red blood cell membrane coated PLGA nanoparticles**

To further evaluate the biocompatibility and the ability to evade immune clearance of RP(P/T), we used coumarin-6 to examine the uptake of macrophages.

Coumarin-6, a hydrophobic green fluorescent indicator, was used to trace the uptake of nanoparticles in tumor cells. C6-NPs and R-C6-NPs were incubated with RAW264.7 for 2 hours. The uptake of C6-NPs and R-C6-NPs by macrophages was studied using CLSM (**Fig. 3A** and **B**). Macrophages incubated with C6-NPs showed strong green fluorescence, while those incubated with R-C6-NPs showed faint green fluorescence. It suggested that the wrapping of the red blood cell membrane could inhibit

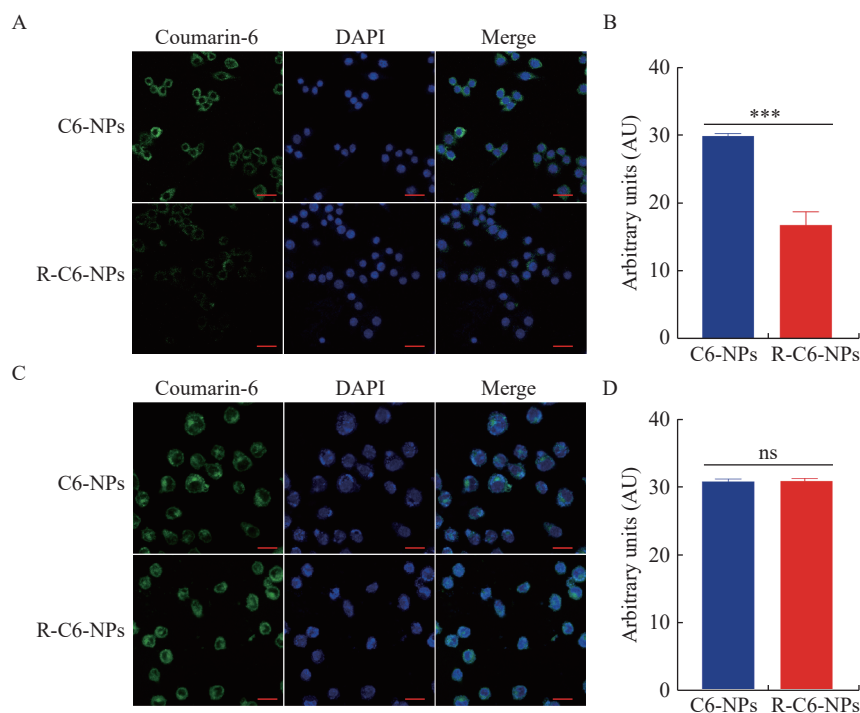


**Fig. 3** Intracellular uptake of red blood cell membrane coated PLGA nanoparticles and naked PLGA nanoparticles. A and B: Uptake of C6-NPs and R-C6-NPs in RAW264.7 cells after 2 hours incubation (A) and quantification of the fluorescent intensity of the intracellular uptake (B). The Student's *t*-test was used to detect statistically significant differences. Error bars indicate SD ( $n=3$ ). \*\*\* $P<0.001$ . C and D: Uptake of C6-NPs and R-C6-NPs in MNK-45 cells (C) and quantification of the fluorescent intensity of the intracellular uptake (D). The Student's *t*-test was used to detect statistically significant differences. Error bars indicate SD ( $n=3$ ). ns: no significant difference. The nucleus was stained with DAPI. The P(P/T) and RP(P/T) were labeled with C6. Scale bars, 20  $\mu\text{m}$ .

the phagocytosis of macrophages. The intracellular uptake of P(P/T) and RP(P/T) were also investigated in MNK-45 cells. The green fluorescence intensity of the R-C6-NP and C6-NP groups were equivalent within MNK45 cells (**Fig. 3C and D**). It indicated that the coating of red blood cell membranes had a negligible effect on the internalization of RP(P/T) in cancer cells.

#### **In vitro cytotoxicity of RP(P/T)**

The cytotoxicity of RP(P/T) against BGC-823 and SGC-7901 was measured by MTT assay. **Fig. 4A–D** show the cell viability of BGC-823 cells incubated with different concentrations of PTX, TPL, P(P/T), RP(P/T) for 24, 48, and 72 hours. Similar to BGC-823, the cell viability of SGC-7901 after exposure to different concentrations of PTX, TPL, P(P/T) RP(P/T) for 24, 48, and 72 hours was shown in **Fig. 4E–H**.

The RP(P/T) has a significant cytotoxic effect on tumor cells in a dose- and time-dependent manner. The formulation groups exhibited comparable or superior cytotoxicity to the free PTX or TPL, especially at low concentrations. With increasing time in culture, differences in cytotoxicity between free drug and formulation groups were exacerbated. Furthermore, the estimated half maximal inhibitory concentration ( $IC_{50}$ ) value of P(P/T) and RP(P/T) (**Table 2**) were significantly lower than that of free PTX, confirming the desirable synergism effect of the two drugs.

#### **In vitro antimetastasis assay of the RP(P/T)**

We then carried out a series of experiments, including the wound healing assay, colony formation assay, and cell invasion assay to analyze the antitumor efficacy of the nanoparticles *in vitro*. First, the colony formation assay was performed to explore the effect of the NPs on the clonogenicity of SGC-7901 cells (**Fig. 5A**). P(P/T) and RP(P/T) exhibited a robust inhibitory effect on the colony-forming ability of cancer cells.

To further examine tumor cell motility, wound-healing assay was conducted (**Fig. 5B**). The migration rate was quantified (**Fig. 5C**). Untreated SGC-7901 cells exhibited significant wound healing ability after 48 hours, demonstrating the strong metastatic properties of gastric cancer cells. Both paclitaxel and triptolide had a slight suppression of the wound healing capacity of the cells. However, P(P/T) and RP(P/T) could remarkably inhibit cell motility compared to free drugs.

Meanwhile, transwell assays on MNK-45 cells were also performed to assess the effect of P(P/T) and RP(P/T) on cell invasion (**Fig. 5D**). The bar graph was

the quantification data of invasion rate (**Fig. 5E**). The results of the invasion were consistent with the migration. The above results demonstrated that the P(P/T) and RP(P/T) had a superior effect in inhibiting cell migration and invasion against free drugs *in vitro*.

## **Discussions**

Paclitaxel, a first-line chemotherapeutic agent, is most commonly used in gastric cancer therapy. It has excellent antitumor effects by increasing polymerization and stability of microtubule but inhibiting the depolymerization of microtubule. However, the drug resistance and poor solubility restricted its clinical application. The combination of chemotherapeutics is an innovative approach to improve clinical outcomes<sup>[22]</sup>. Triptolide, another superior antitumor agent in multiple tumor types, was reported to enhance paclitaxel chemotherapy and reverse drug resistance of PTX<sup>[7]</sup>. However, the above two drugs are hydrophobic and toxic against normal tissues, requiring a smart drug delivery system to increase the solubility, improve efficiency and reduce the toxicity.

The biomimetic system is an innovative strategy for drug delivery. Red blood cell membrane-coated nanoparticles have notable advantages over uncoated ones. These advantages include excellent biocompatibility, low immunogenicity, and a long life span in the circulation, which make them a good candidate for clinical application<sup>[20]</sup>.

In this study, a biomimetic nano-drug delivery system (RP(P/T)), camouflaged with RBCM, was developed to co-load paclitaxel and triptolide. We used a simple emulsion solvent evaporation method to prepare the PLGA core and then cloaked the cell membrane layer by sonication. The preparation of RP(P/T) was confirmed by size, zeta potential, morphology, and protein characterizations, representing by drug loading, encapsulation efficiency, stability, release profile, and cellular uptake assays. Meanwhile, several *in vitro* evaluations, including cytotoxicity assay, colony formation assay, cell migration assay, and cell invasion assay were also performed.

The characterizations conducted verified the successful preparation of RP(P/T). The encapsulation of the red blood cell membrane caused an increase to 117 nm in the particle size and a decrease in the zeta potential to  $-30$  mV. And the designed platform significantly ameliorated the colloidal stability of RP(P/T). When mimicking the blood circulation with 100% FBS, superior circulation stability of the

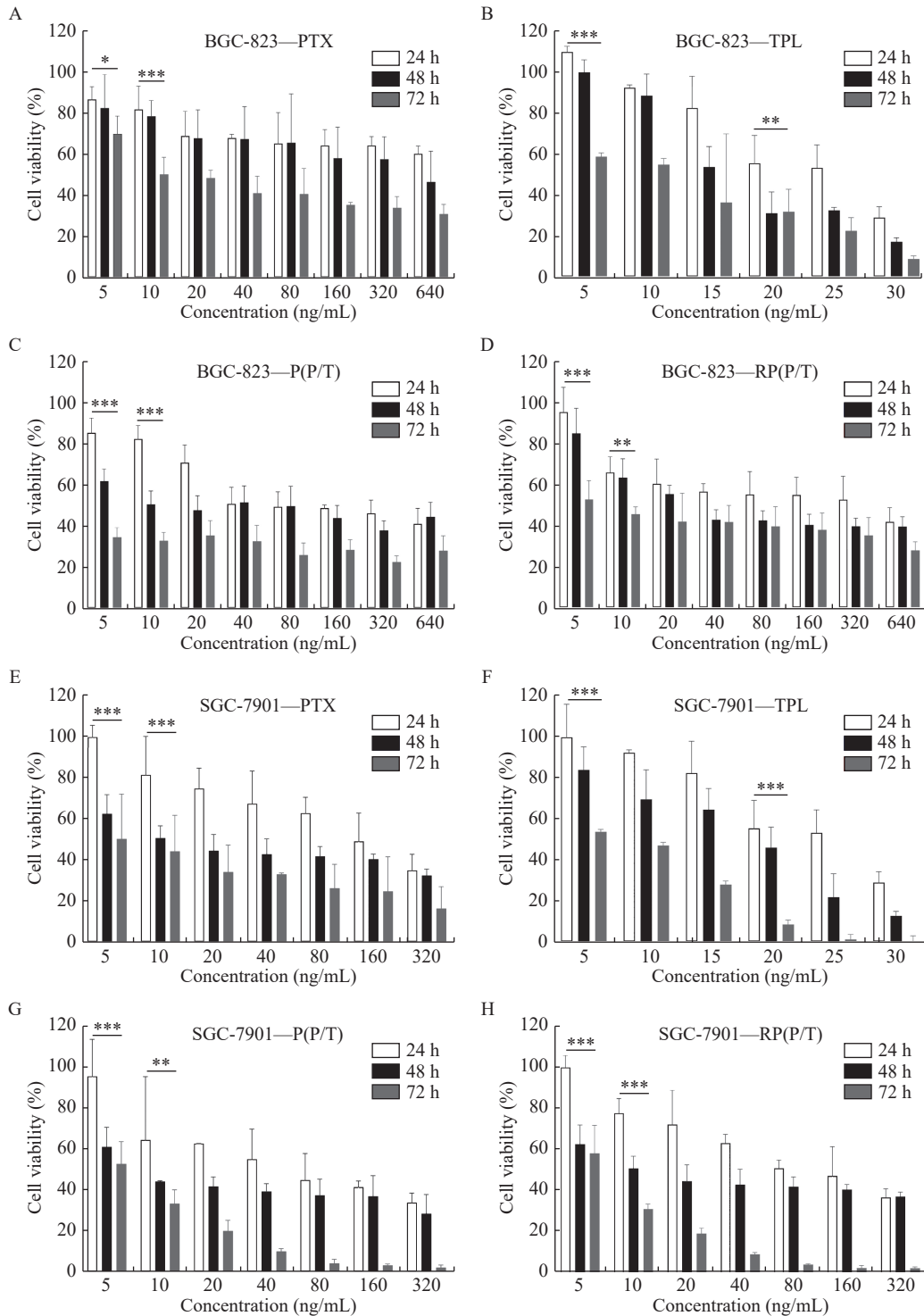


**Fig. 4** *In vitro* anticancer assays of RP(P/T). A–D: After incubation with PTX (A), TPL (B), P(P/T) (C), and RP(P/T) (D) for 24, 48, and 72 hours, cell viability of BGC-823 was evaluated using the MTT assay. BGC-823—PTX, BGC-823—TPL, BGC-823—P(P/T), and BGC-823—RP(P/T) represent the cell viability of BGC-823 after incubation with PTX, TPL, P(P/T), and RP(P/T), respectively. Error bars indicate SD ( $n=3$ ). E–H: After incubation with PTX (E), TPL (F), P(P/T) (G), and RP(P/T) (H) for 24, 48, and 72 hours, the cell viability of SGC-7901 was determined by MTT assay. SGC-7901—PTX, SGC-7901—TPL, SGC-7901—P(P/T), and SGC-7901—RP(P/T) represent the cell viability of SGC-7901 after incubation with PTX, TPL, P(P/T), and RP(P/T), respectively. Error bars indicate SD ( $n=3$ ). The Student's *t*-test was used to detect statistically significant differences between the 24 hours and 72 hours groups. \* $P<0.05$ , \*\* $P<0.01$ , \*\*\* $P<0.001$ . P(P/T): PTX and TPL co-loaded PLGA nanoparticles; RP(P/T): red blood cell membrane coated PTX and TPL co-loaded PLGA nanoparticles; PLGA: poly(lactic-co-glycolic acid); PTX: paclitaxel; TPL: triptolide.

RBCM-coated nanoparticles (RP(P/T)) was observed, which was attributed to the protective effect of red

blood cell membranes during circulation. In addition, the release profile of RP(P/T) in the solution of PBS

**Table 2 The IC<sub>50</sub> of PTX, TPL, P(P/T) and RP(P/T) against BGC-823 and SGC-7901 cells (ng/mL)**

	24 hours		48 hours		72 hours	
	BGC-823	SGC-7901	BGC-823	SGC-7901	BGC-823	SGC-7901
PTX	513.12	153.90	108.98	10.98	10.44	6.18
TPL	25.58	25.58	15.68	18.76	11.04	7.22
P(P/T)	59.96	56.52	23.36	7.87	0.03	4.72
RP(P/T)	379.06 <sup>***</sup>	107.90 <sup>***</sup>	26.92 <sup>***</sup>	10.98 <sup>ns</sup>	6.56 <sup>**</sup>	5.49 <sup>*</sup>

The Student's *t*-test was used to detect statistically significant differences between the PTX and RP(P/T) groups. (ns: no significant difference. \**P*<0.05, \*\**P*<0.01, \*\*\**P*<0.001, *n*=3). PTX: paclitaxel; TPL: triptolide; P(P/T): PTX and TPL-co-loaded PLGA nanoparticles; RP(P/T): red blood cell membrane coated PTX and TPL co-loaded PLGA nanoparticles.

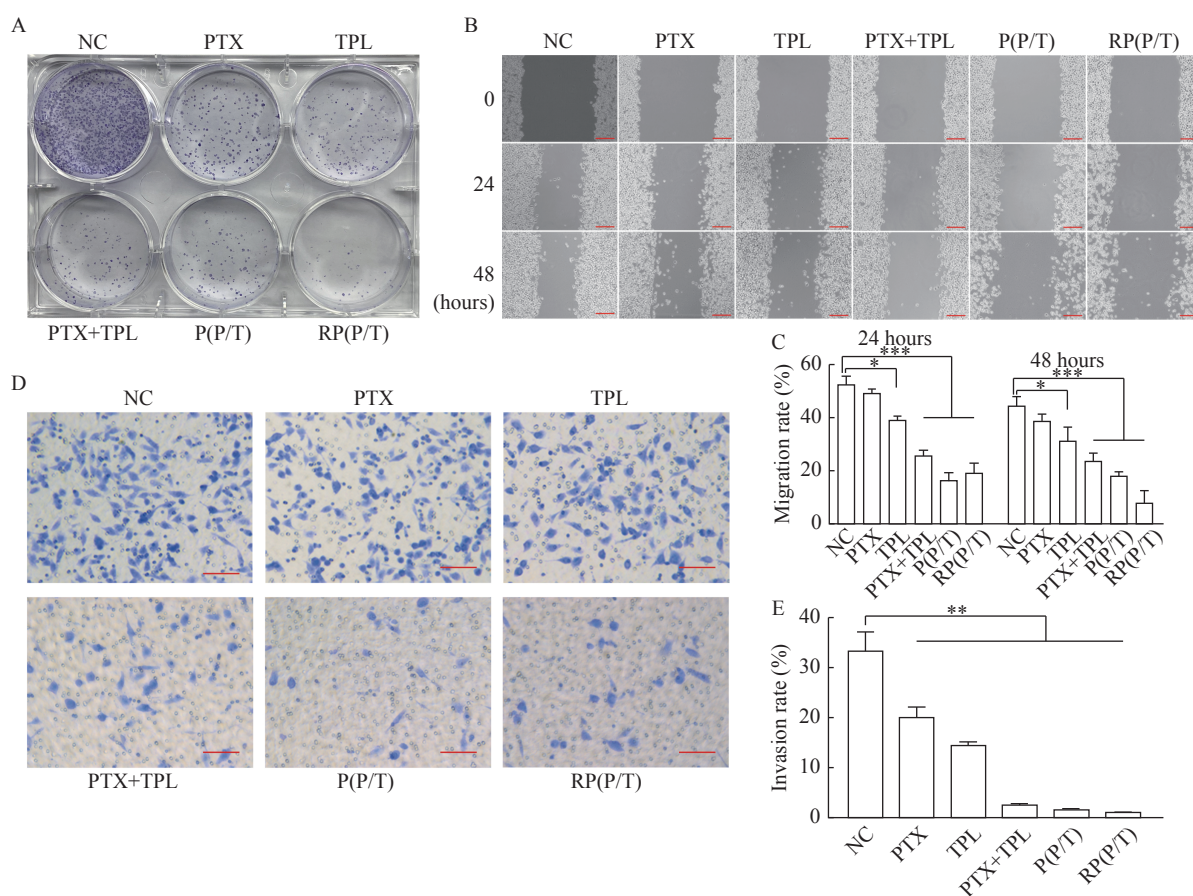


**Fig. 5 In vitro antitumor effect of NPs.** A: The colony formation assay of NC, PTX, TPL, PTX+TPL (the PTX:TPL ratio was 1:0.5), P(P/T), and RP(P/T) against SGC-7901 cells. B: The cell wound healing assay of NC, PTX, TPL, PTX+TPL (the PTX:TPL ratio was 1:0.5), P(P/T), and RP(P/T) against SGC-7901 cells. Scale bar, 200  $\mu$ m. C: Quantitative analysis of the migration ratio. Error bars indicate SD. Student's *t*-test was performed to examine statistically significant differences. \**P*<0.05, \*\*\**P*<0.001, *n*=3. D: Representative images of NC, PTX, TPL, PTX+TPL (the PTX:TPL ratio was 1:0.5), P(P/T) and RP(P/T) on MNK-45 cell invasion. Scale bar, 100  $\mu$ m. E: Quantitative analysis of the invasion ratio. Error bars indicate SD. Student's *t*-test was performed to examine statistically significant differences. \*\**P*<0.01, *n*=3.

(pH 6.5) demonstrated a good potential of RP(P/T) for sustained drug release. In addition, it also suggested that the layer of membrane coating served as a diffusional barrier that could potentially slow down the drug release and increase the stability of the nano-delivery system. So, we deduced that RP(P/T) could longer the residence time and increased the duration of

drugs in the organism<sup>[20]</sup>.

Meanwhile, compared to C6-NPs, the uptake of R-C6-NPs by macrophages was negligible. Proteins on the outer surface of the red blood cell membrane mediate the ability to evade immune-mediated clearance. Among these proteins, CD47, a glycoprotein with a "don't eat me" signal and immune

escape function on the red blood cell membrane, plays a vital role in suppressing phagocytosis<sup>[23]</sup>. CD47 could inhibit phagocytosis by macrophage, prevent normal erythrocytes from being removed by the immune system and enable long-term circulation *in vivo*. As reported previously, we speculate that the "don't eat me" signal CD47 on the red blood cell membrane might limit the phagocytosis of R(P/T) by macrophages<sup>[23]</sup>. The RBCM-coating allowed RP(P/T) to acquire enhanced immune surveillance evasion. And the equal fluorescence intensity between MNK-45 cells treated with C6-NPs and R-C6-NPs indicated that red blood cell membrane cloaking did not affect the cellular uptake of RP(P/T) in cancer cells.

As to *in vitro* evaluations, P(P/T) and RP(P/T) exhibited superior antitumor efficiency than the equivalent dose of free PTX or TPL. In cytotoxicity assay, the combination of paclitaxel and triptolide demonstrated an improved antitumor efficacy (data not shown). It was consistent with prior publications, suggesting the significant synergistic effect of these two drugs. In addition, the P(P/T) and RP(P/T) displayed stronger antitumor activities than free drugs against BGC-823 and SGC-7901 cells owing to the synergistic effect, which might be associated with inhibition of nuclear factor-kappa B (NF- $\kappa$ B) activity<sup>[7]</sup>. The colony formation assay also showed that cell proliferation was severely repressed by RP(P/T).

Gastric cancer is a highly aggressive cancer with a high rate of recurrence and metastasis<sup>[24]</sup>. Wound-healing and transwell assays are commonly used to characterize cell migration and invasion capabilities<sup>[25]</sup>. Profiting from these two assays, we found that RP(P/T) is superior in inhibiting cancer invasion and metastasis compare to the equivalent dose of free PTX or TPL. These results are in accordance with the results found in cytotoxicity assay and colony formation assay. This may be because that triptolide had a strong antimetastatic effect due to the inhibition of expression of matrix metalloproteinases (MMPs), especially MMP7 and MMP19. It was reported that MMPs could mediate extracellular matrix degradation, which is an essential step in tumor invasion and metastasis<sup>[26]</sup>. Thus, our findings are in agreement with previous studies.

Our group has been devoted to developing novel strategies for chemotherapeutic drug delivery. We found that the co-delivery PTX with other anticancer agents (*e.g.*, tetrandrine) could significantly increase the antitumor efficacy of PTX. Our findings were in accordance with the conclusion proved in our previous studies, which demonstrated that combinational

therapies were superior to monotherapy for cancer treatment<sup>[8–9]</sup>.

The highlights of our study include the following: (i) the modification of RBCM; (ii) the combination of paclitaxel and triptolide. First of all, compared with other unmodified nanoparticles in prior publications, RBCM coating offers the following advantages: intrinsic biocompatibility, high biodegradability, long time circulation, low immunogenicity, sustained release, *etc.* Critically, the previous paclitaxel-loaded nano delivery systems showed high immunogenicity and low biocompatibility, while low immunogenicity and high biocompatibility are prerequisites for clinical applications<sup>[27–29]</sup>. In contrast to previously published nanocarriers, the bionic system we developed showed a superior property in long blood circulation by reducing the uptake of macrophages. The long circulation time provided by the RBCM layer might be responsible for the enhanced cytotoxicity of the nanoparticles. Secondly, the combination of paclitaxel and triptolide produced a synergistic effect in gastric cancer cells.

Although *in vitro* experiments are essential to study nano-drug delivery systems, further *in vivo* investigation would be necessary to support the efficacy of this nanoplatform, and follow-up experiments are underway.

In conclusion, our prepared RP(P/T) nanoparticles are more effective in suppressing the growth of gastric cancer cells than free drugs, which illustrates that RP(P/T) might be a potentially better option to promote the therapeutic efficacy of PTX against gastric cancer.

## Acknowledgments

This work was supported by the National Natural Science Foundation of China (No. 82073308 and No. 81773211) and the High-level startup fund of Nanjing Medical University (No. KY109RC2019010).

## References

- [1] Bray F, Ferlay J, Soerjomataram I, et al. Global cancer statistics 2018: GLOBOCAN estimates of incidence and mortality worldwide for 36 cancers in 185 countries[J]. *CA Cancer J Clin*, 2018, 68(6): 394–424.
- [2] Chen W, Sun K, Zheng R, et al. Cancer incidence and mortality in China, 2014[J]. *Chin J Cancer Res*, 2018, 30(1): 1–12.
- [3] China-fact-sheets. The global cancer observatory[EB/OL]. [2020-11-25]. <https://gco.iarc.fr/today/data/factsheets/populations/160-china-fact-sheets.pdf>.
- [4] Ferlay J, Soerjomataram I, Dikshit R, et al. Cancer incidence and mortality worldwide: sources, methods and major patterns

- in GLOBOCAN 2012[J]. *Int J Cancer*, 2015, 136: E359–386.
- [5] NCCN guidelines for patients®: stomach cancer[EB/OL]. [2019-06-22]. <https://www.nccn.org/patients/guidelines/content/PDF/stomach-patient.pdf>.
- [6] Efferth T, Li PCH, Konkimalla VS, et al. From traditional Chinese medicine to rational cancer therapy[J]. *Trends Mol Med*, 2007, 13(8): 353–361.
- [7] Wang W, Lin W, Wang Q, et al. The enhanced antitumor effect of combined triptolide and paclitaxel on pancreatic cancer cell lines[J]. *J Clin Oncol*, 2014, 32(S3): 335.
- [8] Li X, Lu X, Xu H, et al. Paclitaxel/tetrandrine coloaded nanoparticles effectively promote the apoptosis of gastric cancer cells based on "oxidation therapy"[J]. *Mol Pharmaceut*, 2012, 9(2): 222–229.
- [9] Li X, Yu N, Li J, et al. Novel "carrier-free" nanofiber codelivery systems with the synergistic antitumor effect of paclitaxel and tetrandrine through the enhancement of mitochondrial apoptosis[J]. *ACS Appl Mater Interfaces*, 2020, 12(9): 10096–10106.
- [10] Chen S, Dai Y, Zhao J, et al. A mechanistic overview of triptolide and celastrol, natural products from *Tripterygium wilfordii* Hook F[J]. *Front Pharmacol*, 2018, 9: 104.
- [11] Roy V, LaPlant BR, Gross GG, et al. Phase II trial of weekly nab (nanoparticle albumin-bound)-paclitaxel (nab-paclitaxel) (Abraxane®) in combination with gemcitabine in patients with metastatic breast cancer (N0531)[J]. *Ann Oncol*, 2009, 20(3): 449–453.
- [12] Couvreur P. Nanoparticles in drug delivery: past, present and future[J]. *Adv Drug Deliv Rev*, 2013, 65(1): 21–23.
- [13] Wang L, Jia E. Ovarian cancer targeted hyaluronic acid-based nanoparticle system for paclitaxel delivery to overcome drug resistance[J]. *Drug Deliv*, 2016, 23(5): 1810–1817.
- [14] Ahmed F, Pakunlu RI, Brannan A, et al. Biodegradable polymersomes loaded with both paclitaxel and doxorubicin permeate and shrink tumors, inducing apoptosis in proportion to accumulated drug[J]. *J Control Release*, 2006, 116(2): 150–158.
- [15] Xu H, Lu X, Li J, et al. Superior antitumor effect of extremely high drug loading self-assembled paclitaxel nanofibers[J]. *Int J Pharmaceut*, 2017, 526(1-2): 217–224.
- [16] Farokhzad OC, Langer R. Impact of nanotechnology on drug delivery[J]. *ACS Nano*, 2009, 3(1): 16–20.
- [17] Patra JK, Das G, Fraceto LF, et al. Nano based drug delivery systems: recent developments and future prospects[J]. *J Nanobiotechnol*, 2018, 16(1): 71.
- [18] Hu C, Zhang L, Aryal S, et al. Erythrocyte membrane-camouflaged polymeric nanoparticles as a biomimetic delivery platform[J]. *Proc Natl Acad Sci USA*, 2011, 108(27): 10980–10985.
- [19] Kroll AV, Fang R, Zhang L. Biointerfacing and applications of cell membrane-coated nanoparticles[J]. *Bioconjugate Chem*, 2017, 28(1): 23–32.
- [20] Fang R, Kroll AV, Gao W, et al. Cell membrane coating nanotechnology[J]. *Adv Mater*, 2018, 30(23): 1706759.
- [21] Tang C, Wang C, Zhang Y, et al. Recognition, intervention, and monitoring of neutrophils in acute ischemic stroke[J]. *Nano Lett*, 2019, 19(7): 4470–4477.
- [22] Hu Q, Sun W, Wang C, et al. Recent advances of cocktail chemotherapy by combination drug delivery systems[J]. *Adv Drug Deliv Rev*, 2016, 98: 19–34.
- [23] Oldenborg PA, Zheleznyak A, Fang YF, et al. Role of CD47 as a marker of self on red blood cells[J]. *Science*, 2000, 288(5473): 2051–2054.
- [24] Li W, Ng JMK, Wong C, et al. Molecular alterations of cancer cell and tumour microenvironment in metastatic gastric cancer[J]. *Oncogene*, 2018, 37(36): 4903–4920.
- [25] Long Y, Lu Z, Mei L, et al. Enhanced melanoma-targeted therapy by "Fru-Blocked" phenylboronic acid-modified multiphase antimetastatic micellar nanoparticles[J]. *Adv Sci*, 2018, 5(11): 1800229.
- [26] Zhao H, Yang Z, Wang X, et al. Triptolide inhibits ovarian cancer cell invasion by repression of matrix metalloproteinase 7 and 19 and upregulation of E-cadherin[J]. *Exp Mol Med*, 2012, 44(11): 633–641.
- [27] Sun B, Taha MS, Ramsey B, et al. Intraperitoneal chemotherapy of ovarian cancer by hydrogel depot of paclitaxel nanocrystals[J]. *J Control Release*, 2016, 235: 91–98.
- [28] Liu Y, Ng Y, Toh MR, et al. Lipid-dendrimer hybrid nanosystem as a novel delivery system for paclitaxel to treat ovarian cancer[J]. *J Control Release*, 2015, 220: 438–446.
- [29] Peng J, Chen J, Xie F, et al. Herceptin-conjugated paclitaxel loaded PCL-PEG worm-like nanocrystal micelles for the combinatorial treatment of HER2-positive breast cancer[J]. *Biomaterials*, 2019, 222: 119420.